

We are IntechOpen, the world's leading publisher of Open Access books Built by scientists, for scientists

6,900

Open access books available

185,000

International authors and editors

200M

Downloads

Our authors are among the

154

Countries delivered to

TOP 1%

most cited scientists

12.2%

Contributors from top 500 universities



WEB OF SCIENCE™

Selection of our books indexed in the Book Citation Index
in Web of Science™ Core Collection (BKCI)

Interested in publishing with us?
Contact book.department@intechopen.com

Numbers displayed above are based on latest data collected.
For more information visit www.intechopen.com



Flight Vehicle Performance

Aram Baghiyan

Abstract

In this chapter, the problem of flight vehicle performance is described. Performance parameters, such as lift-to-drag ratio, maximum and minimum level flight speed, speeds for the best rate of climb, steepest climb, maximum range and endurance, and most economical climb are described using graphical methods, such as drag polar, Zhukovsky curves with combination of analytical derivations. The approach of graphical description of flight vehicle performance allows to understand the physical basics of the aerodynamic properties of flight vehicles easier and to develop deeper connectivity between their interpretations. In addition, flight envelope and operational limits are discussed using both analytical and graphical methods for better understanding.

Keywords: aerodynamics, flight vehicle, drag polar, flight performance, Zhukovsky curves

1. Introduction

During the flight, aircraft is usually loaded by four forces (**Figure 1**)—gravity force G , lift L , drag D , and thrust T . The combination of these forces defines the behavior of flight and the performance of aircraft. There are also cases when the side forces S act on aircraft due to sideslip (**Figure 1**), which are balanced by the vertical tail of aircraft, and during the analysis of the flight vehicle performance they are usually neglected.

As we can see from the **Figure 1**, the vector of aircraft speed \vec{v} does not coincide with its body frame axes x_b, y_b , and z_b and has inclinations from axis x_b expressed by flow angles—angle of attack α and sideslip angle β . The point of acting gravity force is the center of gravity O_{cg} and usually the line of acting of thrust passes through the center of gravity to avoid generation of destabilizing torques or moments. Aerodynamic forces act at the point named center of pressure O_{cp} , which is not a fixed and changes its position depending on the angle of attack and the air speed. Therefore, a more stable point—aerodynamic center O_{ac} —is introduced, where the changes of aerodynamic forces act, so the aerodynamic moments at that point do not change with the changes of angle of attack. However, aerodynamic center can have variations [1] with Mach number $M = v/a$, where v is the magnitude of aircraft speed, a is the local speed of sound.

In problems of flight vehicle performance analysis, usually a simpler model of the balance of forces is used: the side forces S are neglected due to small values of sideslip angle β in steady flight regimes, the point of action of all unneglectable forces assumed the same, at the same time, taking the lines of action of thrust T and drag D forces coinciding (**Figure 2**).

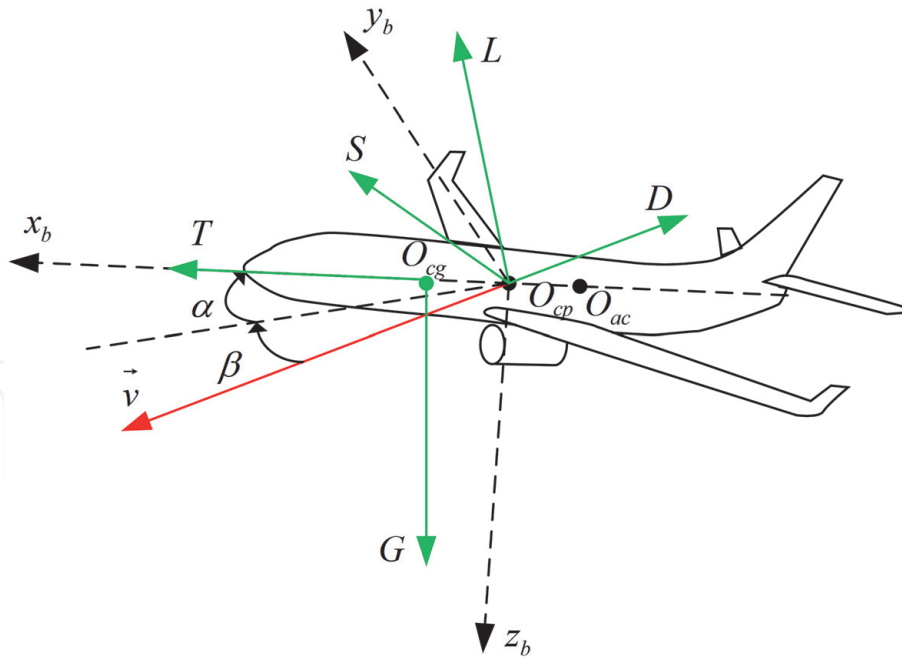


Figure 1.
Forces acting on aircraft.

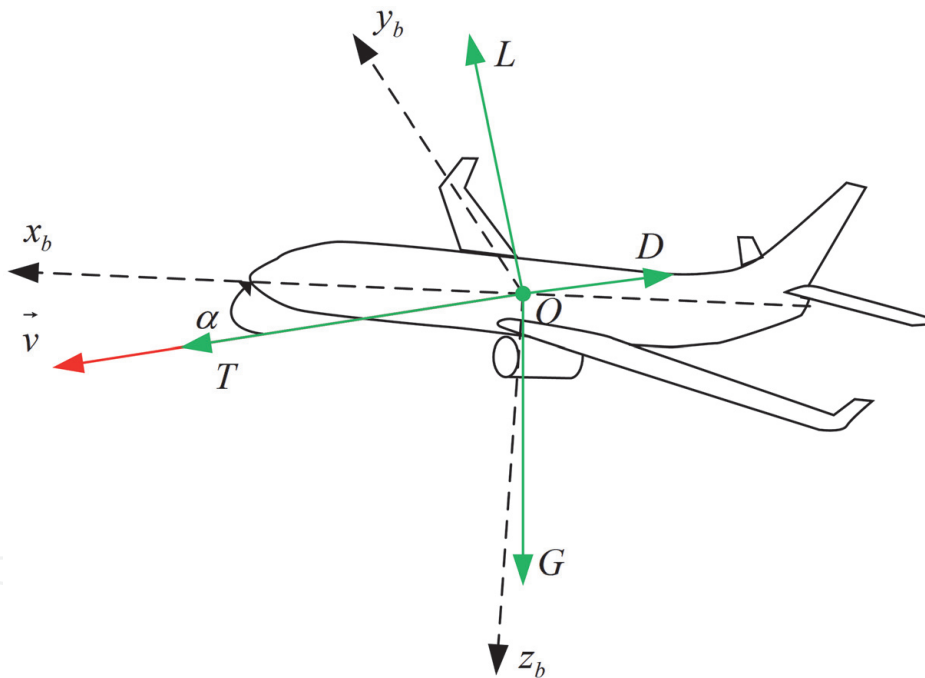


Figure 2.
Simple model of force balance.

Based on the model of force balance, we will study flight vehicle performance at several steady flight regimes, but before getting there let us consider the aerodynamic forces—lift and drag, and the effect of their relations on the aerodynamic quality of aircraft.

2. Drag polar of aircraft

Taking as a reference any paper on aerodynamics, we can find the formulas for lift L and drag D forces [2]:

$$\begin{cases} L = c_L \frac{\rho v^2}{2} S_{ref}, \\ D = c_D \frac{\rho v^2}{2} S_{ref}, \end{cases} \quad (1)$$

where c_L is the dimensionless lift coefficient; ρ is the freestream density; v is the magnitude of freestream speed, which is taken equal to aircraft speed; S_{ref} is the reference area, and c_D is the dimensionless drag coefficient.

From the system of Eq. (1)

$$\frac{L}{D} = \frac{c_L}{c_D}.$$

The ratio $k = L/D$ is usually called lift-to-drag ratio and in eastern literature it is defined as aerodynamic quality of aircraft. This ratio has interesting properties and it changes with changes of angle of attack α .

Let us consider now the lift coefficient c_L and its relations with angle of attack α (**Figure 3**), which is similar to the analogous relation for 2-D airfoils. The function $c_L = f_L(\alpha)$ can be found using experiments with aircraft model in wind tunnels or using methods of computational fluid dynamics (CFD).

As we can see from the graph of function $c_L = f_L(\alpha)$ (**Figure 3**) there is an angle of attack α_{cr} at which the lift coefficient is maximal, that is, c_{Lmax} . The flight at critical angle of attack α_{cr} will lead to stall, resulting aircraft crash. At angle of attack α_{ts} , the tip stall processes are started and the rate of increase of lift coefficient is decelerated, allowing it to get its maximum value c_{Lmax} and decrease sufficiently. At the point (α_{ts}, c_{Lts}) of starting tip stall, the effects of shaking of aircraft are started [3]. The range between angles of attack α_0 , which is called zero lift angle of attack,

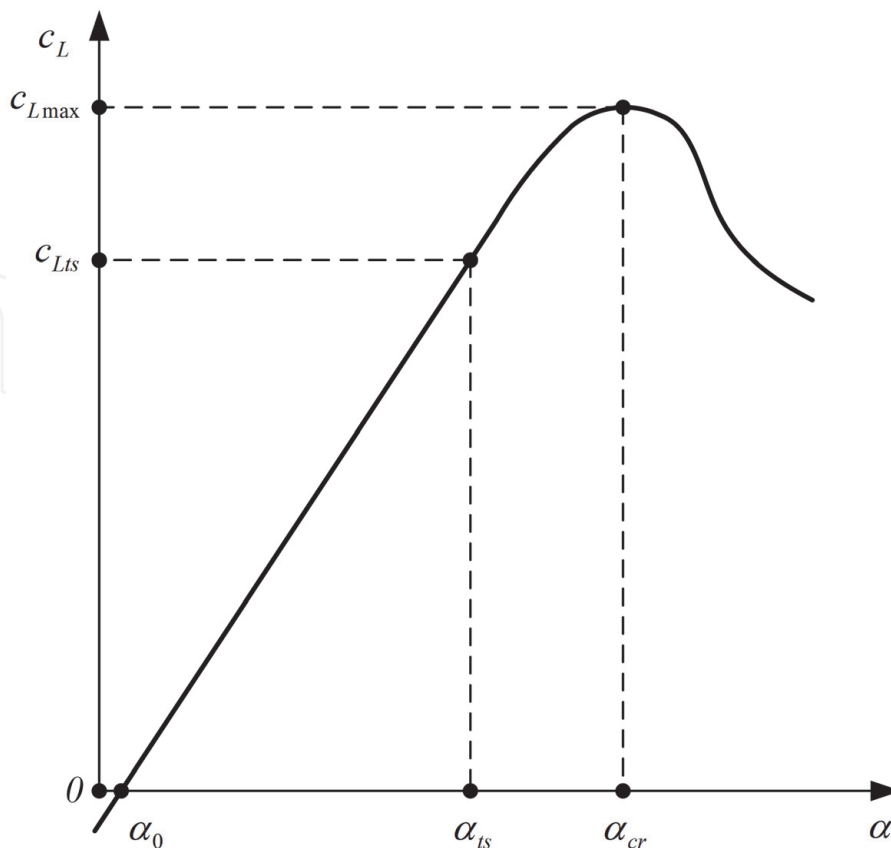


Figure 3.
 Lift coefficient of aircraft versus angle of attack.

and α_{ts} is the range of regular flights of aircraft and as it can be observed at this range the function $c_L = f_L(\alpha)$ is linear.

Before getting to the drag coefficient study, let us consider the existing types of the drag force. The drag force D can be represented as a sum of parasitic drag D_p , which consists of form drag D_f and skin friction drag D_{sf} [4], lift-induced D_i drag, wave drag D_w , and interference drag D_{if} :

$$D = D_f + D_{sf} + D_i + D_w + D_{if},$$

or, which is the same as

$$c_D \frac{\rho v^2}{2} S_{ref} = (c_{Dp} + c_{Di} + c_{Dw} + c_{Dif}) \frac{\rho v^2}{2} S_{ref},$$

where $c_{Dp} = c_{Df} + c_{Dsf}$ is the parasitic drag coefficient, c_{Df} is the form drag coefficient, c_{Dsf} is the skin friction drag coefficient, c_{Di} is the lift-induced drag coefficient, c_{Dw} is the wave drag coefficient, and c_{Dif} is the inference drag coefficient.

Parasitic drag is the pressure difference in front of and behind the wing. The pressure difference depends on the shape of the wing airfoil, its relative thickness \bar{c} and curvature. The larger the relative thickness of the wing airfoil, the greater the form drag (also known as pressure drag); on the other hand, the lower the relative thickness of the wing airfoil, the greater the effect of skin friction drag [5] (**Figure 4**).

The lift-induced drag is the result of the flow tilt (**Figure 5**). Due to the pressure difference above and under the wing on its tips, vortices are generated, leading to the downwash of air from upper surface with velocity u . Thus the effective flow speed v_{eff} becomes the vector sum of the freestream air speed v and downwash speed u . The direction of the effective flow speed differs from the freestream velocity's direction by angle $\delta\alpha$, so the effective angle of attack α_{eff} is defined as:

$$\alpha_{eff} = \alpha + \delta\alpha.$$

With an increase in the angle of attack or lift coefficient, the pressure difference under and above the wing increases quickly, and the coefficient of lift-induced drag increases according to the quadratic law [2]:

$$c_{Di} = \frac{c_L^2}{\pi \lambda e}, \quad (2)$$

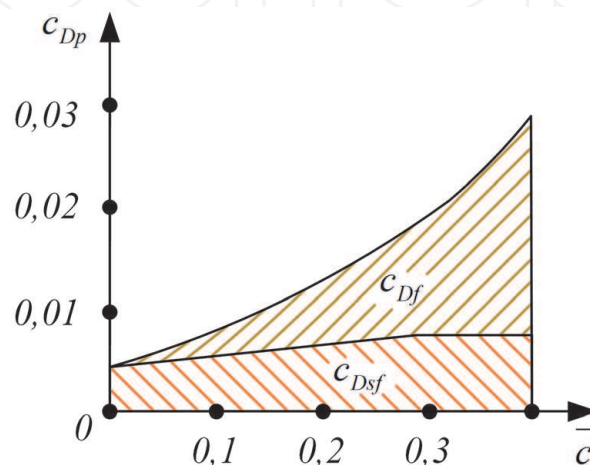


Figure 4.
Parasitic drag components.

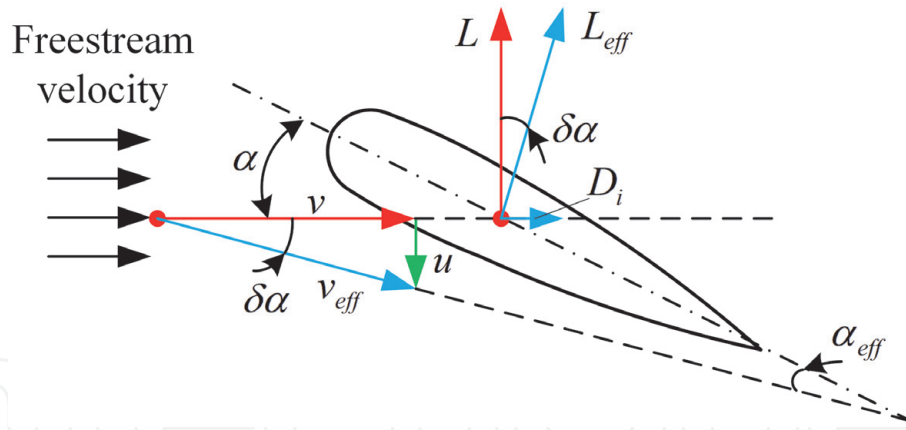


Figure 5.
 On lift-induced drag.

where $\lambda = b^2/S_{ref}$ is the aspect ratio, b is the wing span, S_{ref} is the wing reference area, and e is the span efficiency.

The wave drag D_w is a consequence of the compressibility of the air and occurs when there are shock waves near the aircraft.

The mutual influence of the parts of the aircraft is called interference. It occurs due to a change in the velocity field, as a result of which the nature of the flow around the aircraft changes leading to generation of interference drag D_{if} .

Based on the review of drag components, we can divide them into components related to the lift generation or lift-induced drag, and components not related to the lift generation:

$$c_D = c_{D0} + c_{Di}, \quad (3)$$

where c_{D0} is the component of drag coefficient not related with the lift generation and is called zero lift drag coefficient. Usually c_{D0} is taken as constant and not related to the angle of attack, while c_{Di} is proportional to the square of lift coefficient c_L , which linearly depends on angle of attack α in range of the regular flight regimes. Thus the function $c_D = f_D(\alpha)$ should have the graph of parabolic form (Figure 6).

Similar to $c_L = f_L(\alpha)$, function $c_D = f_D(\alpha)$ can be found using experiments with aircraft model in wind tunnels and using CFD tools.

Using estimated or experimental results for $f_L(\alpha)$ and $f_D(\alpha)$ at set of angles of attack, it is possible to draw drag polar of aircraft (Figure 7).

Based on the drag polar conditions for the best lift-to-drag ratio, zero lift drag and maximal lift can be found. By drawing tangent 1 to the curve of drag polar from the origin of coordinate frame $c_D c_L$, the best lift-to-drag ratio can be found, which corresponds to the angle of attack α_{bldr} ; the tangent 2 to the drag polar parallel to axis c_D defines maximal value of lift coefficient $c_{L_{max}}$ at critical angle of attack α_{cr} , and tangent 3 to the drag polar parallel to axis c_L defines zero lift drag coefficient c_{D0} at zero lift angle of attack α_0 .

The angle of attack α_{bldr} of best lift-to-drag ratio has sufficient role in the flight of aircraft, as the flight with this angle provides the maximum value of the mentioned ratio, also known as aerodynamic quality of aircraft:

$$k_{max} = \frac{f_L(\alpha_{bldr})}{f_D(\alpha_{bldr})}.$$

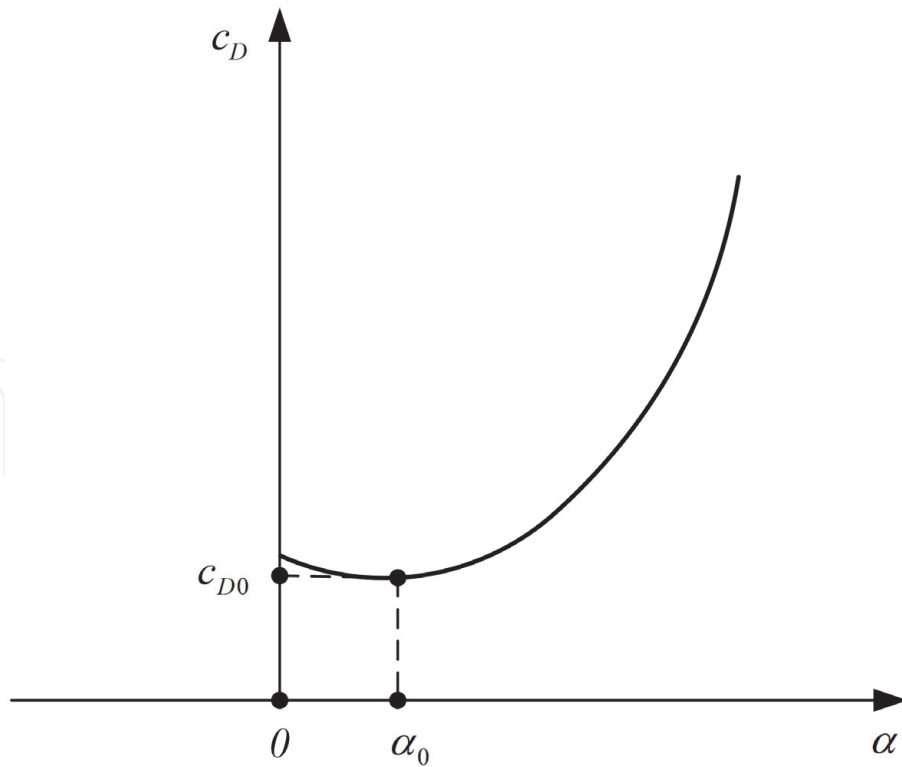


Figure 6.
Drag coefficient of aircraft versus angle of attack.

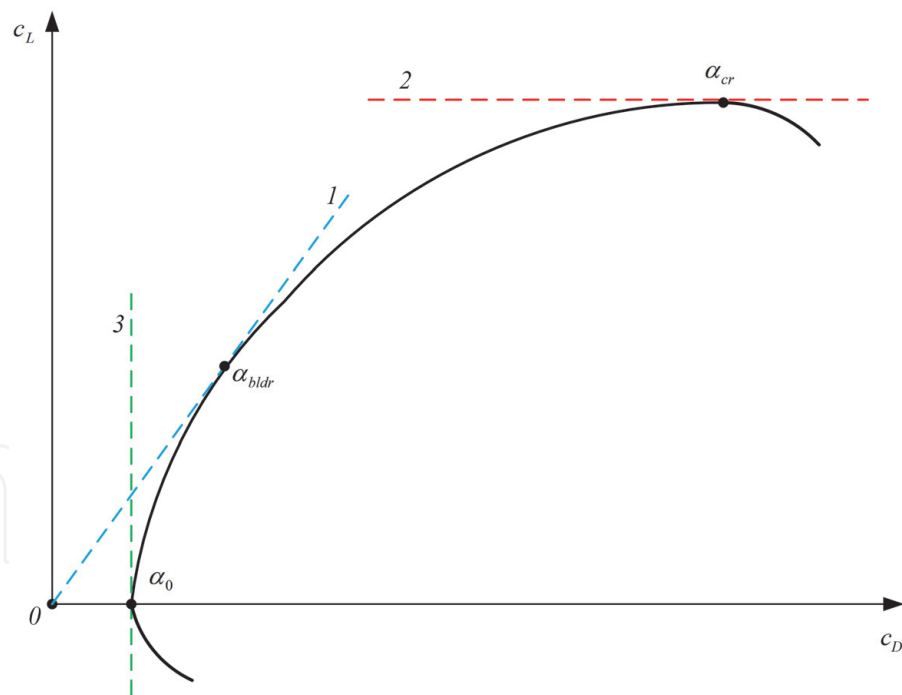


Figure 7.
Drag polar of aircraft.

Let us consider Eq. (3) taking into account Eq. (2):

$$c_D = c_{D0} + \frac{c_L^2}{\pi \lambda e}$$

The above expression is also called drag polar equation, with the use of which we can represent the non-negative values of lift coefficient as

$$c_L = \sqrt{\pi\lambda e(c_D - c_{D0})}.$$

Taking c_D derivative of c_L we get:

$$\frac{\partial c_L}{\partial c_D} = \partial \frac{\sqrt{\pi\lambda e(c_D - c_{D0})}}{\partial c_D} = \frac{\pi\lambda e}{2\sqrt{\pi\lambda e(c_D - c_{D0})}}.$$

At point $c_D(\alpha_{bldr})$, this derivative is the same as the slope k_{\max} of tangent 1 from **Figure 7**, so we can write down the following expression:

$$\frac{\pi\lambda e}{2\sqrt{\pi\lambda e(c_D(\alpha_{bldr}) - c_{D0})}} = \frac{c_L(\alpha_{bldr})}{c_D(\alpha_{bldr})} = \frac{\sqrt{\pi\lambda e(c_D(\alpha_{bldr}) - c_{D0})}}{c_D(\alpha_{bldr})},$$

which can be easily transformed to

$$c_D(\alpha_{bldr}) = 2c_{D0}. \quad (4)$$

Based on the Eq. (4) we can find the maximal value of lift-to-drag ratio:

$$k_{\max} = \frac{1}{2} \sqrt{\frac{\pi\lambda e}{c_{D0}}}.$$

To examine the dependency of the lift-to-drag ratio on angles of attack, the graph of the function $k(\alpha) = f_L(\alpha)/f_D(\alpha)$ can be plotted (**Figure 8**) and the range of angles near the α_{bldr} studied to find the effective flight regimes and patterns [3, 6].

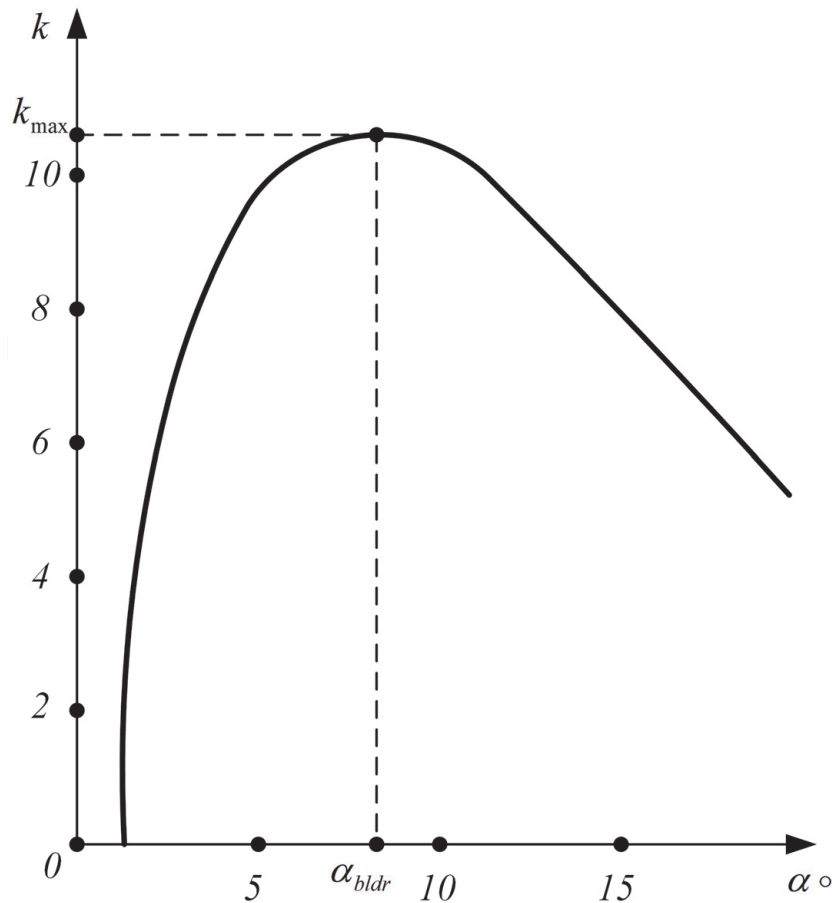


Figure 8.
 Lift-to-drag ratio versus angle of attack.

Examined material is one of core bases of aircraft performance, and the results obtained through the above analysis are used in studies of different flight paths and patterns and will be referred in next subsection dedicated to the Zhukovsky curves.

3. Zhukovsky curves

Let us now consider steady horizontal flight. The scheme on **Figure 2** will be transformed to the following form (**Figure 9**):

In steady horizontal flight, we have the following equation of the force balance:

$$\begin{cases} L = G, \\ T = D. \end{cases} \quad (5)$$

which is same as:

$$\begin{cases} c_L \frac{\rho v^2}{2} S_{ref} = G, \\ T = c_D \frac{\rho v^2}{2} S_{ref} = \left(c_{D0} + \frac{c_L^2}{\pi \lambda e} \right) \frac{\rho v^2}{2} S_{ref}. \end{cases}$$

From the first equation of the above system, we can find that

$$c_L = \frac{2G}{\rho v^2 S_{ref}},$$

and by substituting the value c_L in the second equation we get:

$$T = c_{D0} \frac{\rho v^2}{2} S_{ref} + \frac{1}{\pi \lambda e} \frac{2G^2}{\rho v^2 S_{ref}}.$$

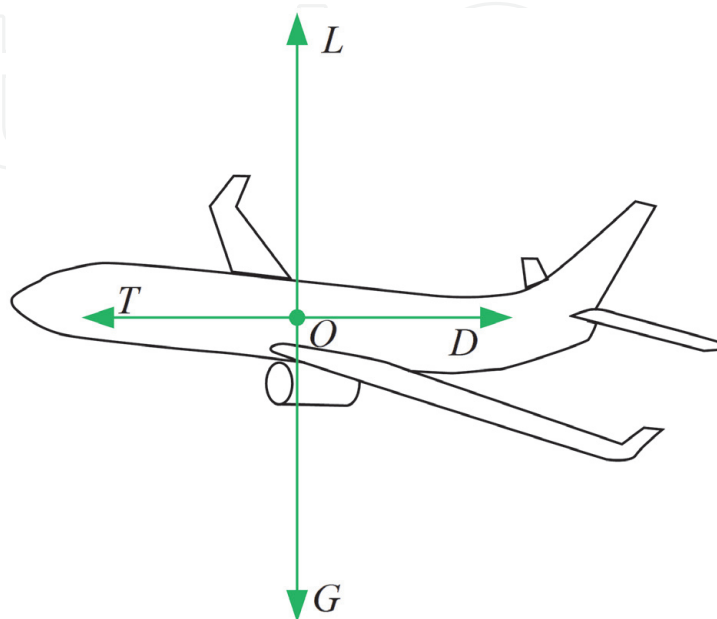


Figure 9.
Force balance at steady horizontal flight.

Based on the above result, we can state that the required thrust T_r for the steady horizontal flight should be equal to the sum of zero lift drag D_0 and lift-induced drag D_i , which are defined as:

$$\begin{cases} T_r = D_0 + D_i, \\ D_0 = c_{D0} \frac{\rho v^2}{2} S_{ref}, \\ D_i = c_{Di} \frac{\rho v^2}{2} S_{ref} = \frac{1}{\pi \lambda e} \frac{2G^2}{\rho v^2 S_{ref}}. \end{cases}$$

As we can see, zero lift drag D_0 is proportional to the square of the air speed, while lift-induced drag D_i is inversely proportional to the square of air speed.

Let us now define the conditions of minimal drag or, which is the same as, minimal required thrust at steady horizontal flight:

$$\frac{\partial T_r}{\partial v} = 2c_{D0} \frac{\rho v}{2} S_{ref} - 2 \frac{1}{\pi \lambda e} \frac{2G^2}{\rho v^3 S_{ref}} = 0.$$

The above expression can be rewritten as:

$$c_{D0} \frac{\rho v^2}{2} S_{ref} = \frac{1}{\pi \lambda e} \frac{2G^2}{\rho v^2 S_{ref}}. \quad (6)$$

It is obvious that the left-hand side of the above is zero lift drag D_0 and the right-hand side is lift-induced drag D_i :

$$D_0 = D_i,$$

or

$$c_{D0} = c_{Di}.$$

Thus, the drag coefficient is equal:

$$c_D = c_{D0} + c_{Di} = 2c_{D0}.$$

As we remember from the drag polar, the same condition is true for maximal lift-to-drag ratio, so the conditions for minimal required thrust and maximal lift-to-drag ratio are the same. To complete the calculations of all parameters for minimal required thrust, let us derive the expressions for lift coefficient and air speed:

$$c_{Di} = c_{D0} = \frac{c_L^2}{\pi \lambda e},$$

so,

$$c_L = \sqrt{\pi \lambda e c_{D0}},$$

and from Eq. (6)

$$v_{(L/D) \min} = \sqrt[4]{\frac{1}{\pi \lambda e c_{D0}} \frac{4G^2}{\rho^2 S_{ref}^2}}.$$

We can also find the characteristics of available thrust T_a provided by manufacturers of engines or the estimations of available thrust from the sources of literature. In [7, 8], the forms of dependency of available thrust on the air speed for several types of engines are presented. Particularly, in [3] we can find available thrust versus air speed at several altitudes for the jet aircraft L-39 (**Figure 10**).

Based on the available information, Nikolay Zhukovsky developed a graphical method for the analysis of the range of the horizontal flight speeds at different altitudes. His method is based on the plotting curves of zero lift drag and lift-induced drag versus air speed at different altitudes, graphically calculating their sum, and plotting the dependencies of available thrust on air speed at corresponding altitudes for graphoanalytic estimation of ranges of available air speeds for horizontal flight at different altitudes. The set of curves obtained through the above-described procedure in memory of him are called Zhukovsky curves. The graph with curves of required and available thrusts or powers at certain altitude is also called performance diagram.

Let us implement the method proposed Zhukovsky for any altitude, for example, do a plot for the altitude of zero meters above sea level (**Figure 11**) and define the speed characteristics of the horizontal flight.

From Zhukovsky curves at sea level altitude, we can find the maximum speed v_{\max} corresponding to the right point of intersection of curves for required thrust $T_r(v)$ and available thrust $T_a(v)$. At speed $v_{(L/D)\min}$ for which zero lift drag becomes equal to lift-induced drag, $D_0(v_{(L/D)\min}) = Di(v_{(L/D)\min})$, we get minimal required thrust $T_{r\min} = 2D_0(v_{(L/D)\min}) = 2Di(v_{(L/D)\min})$. This speed is a very important

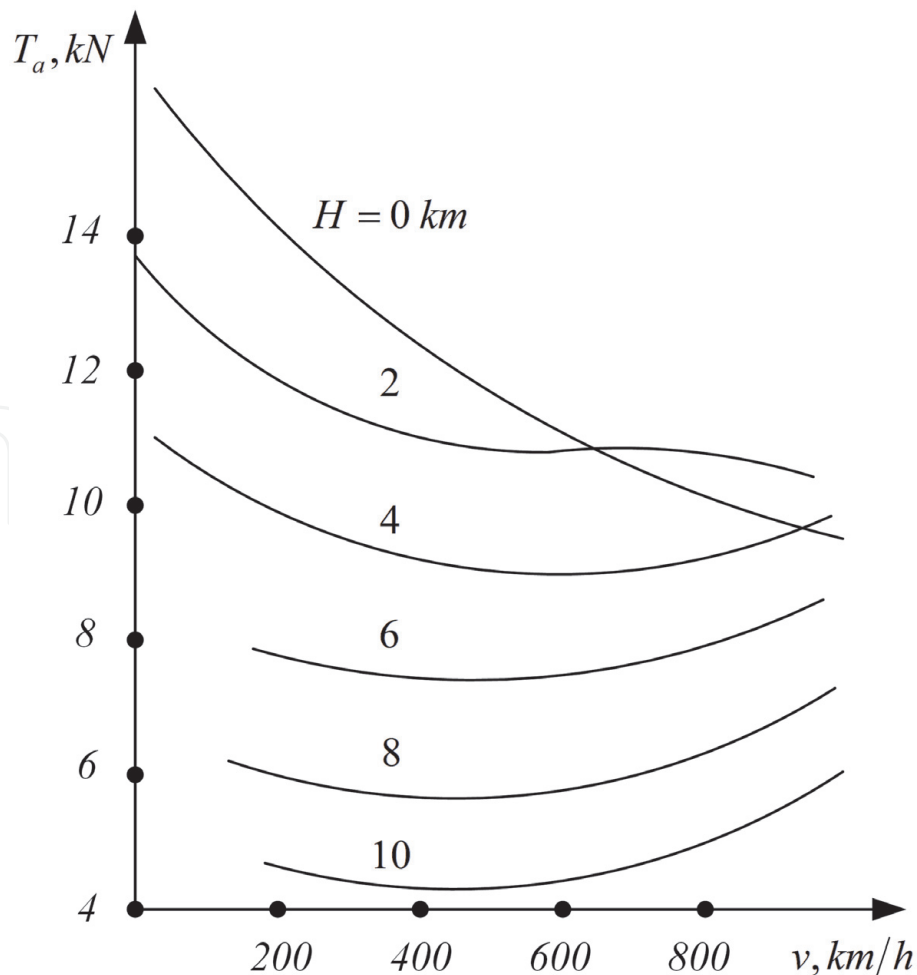


Figure 10.
Available thrust for jet aircraft L-39.

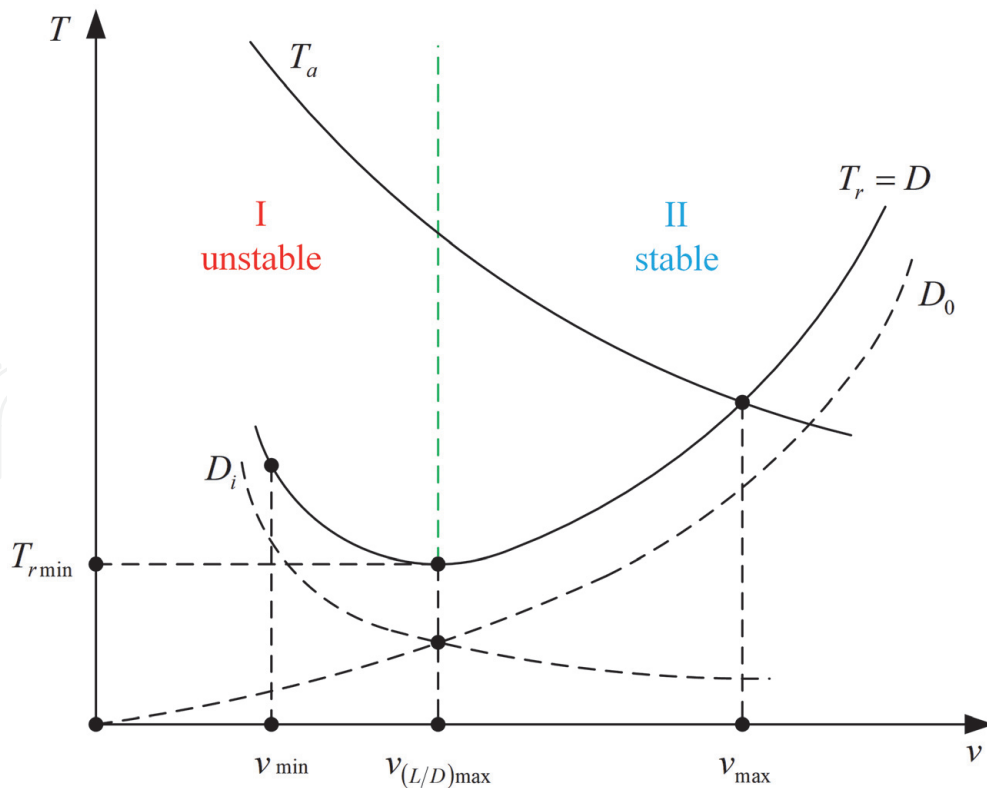


Figure 11.
 Zhukovsky curves at sea level altitude.

quantity from the point of horizontal flight, as the flight at lower speeds is not stable to the accidental changes of speed and requires attention of pilots. On the other hand, the flight at higher speeds than $v_{(L/D) \min}$ is stable to accidental changes of speed, as if speed decreases drag force also decreases and as the thrust was at initial value it accelerates the aircraft till there is a balance between thrust and drag. We get a similar picture for accidental increase of speed at stable region II, for which the drag force decelerates the aircraft till drag-thrust balance. For unstable region I, the dangerous case is the accidental decrease of speed, which increases drag leading to decelerating the aircraft till stall. To fly at unstable region of speeds, the pilot needs always to work with the throttle to increase thrust when it is required. Minimum speed v_{\min} at sea level flight is not defined from the above curves and refers to the stall speed, which can be found from the condition of required lift:

$$c_{L \max} \frac{\rho v^2}{2} S_{ref} = G,$$

or

$$v_{\min} = \sqrt{\frac{2G}{c_{L \max} \rho S_{ref}}}.$$

For flight at higher altitudes, we can get conditions when the required thrust at the above minimum speed is much higher than the available thrust at that altitude (**Figure 12**). In such cases, minimum speed defined as minimum thrust speed $v_{T \min}$ corresponds to the left point of intersection of curves for required thrust $T_r(v)$ and available thrust $T_a(v)$.

The idea of plotting Zhukovsky curves at sea level flight allows us to have the same graph at any altitude H for the required thrust $T_r(v_{IAS})$ versus indicated

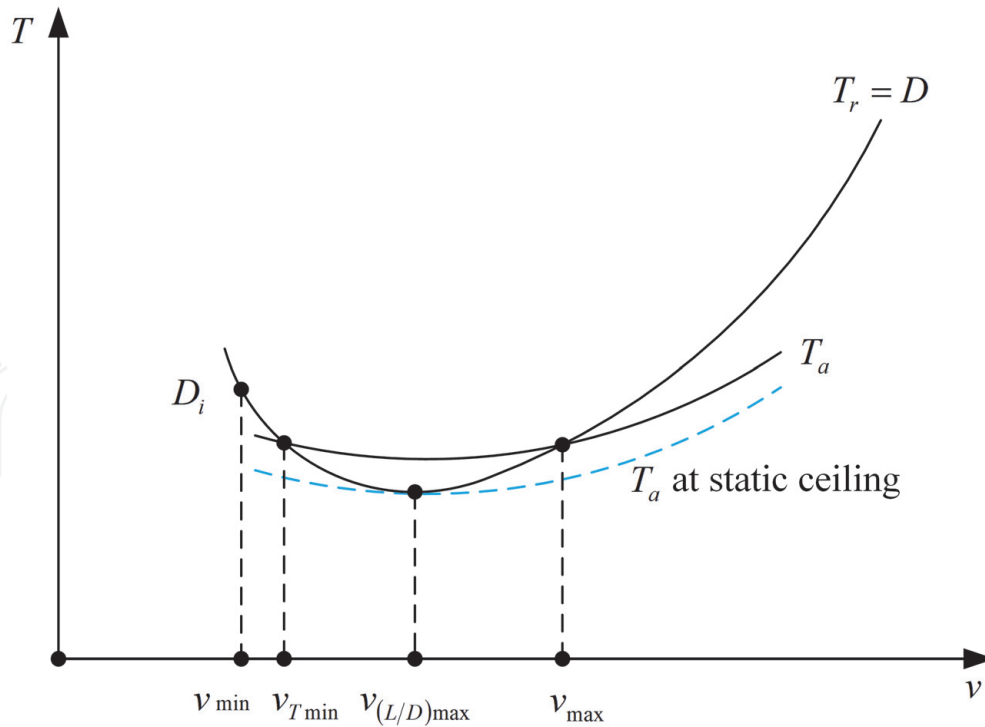


Figure 12.
On minimum thrust speed.

airspeed (IAS), which is usually measured on aircraft and related to the true airspeed (TAS) v_{TAS} via the expression:

$$v_{IAS} = v_{TAS} \sqrt{\frac{\rho_H}{\rho_0}},$$

where ρ_0 is the air density at sea level and ρ_H is the air density at altitude H above sea level (ASL).

Based on the Zhukovsky curves based on IAS, we can define the theoretical or static ceiling of horizontal flight (**Figure 12**), which is an altitude where the horizontal flight is possible only with IAS equal to $v_{(L/D)min}$. The service ceiling has a more practical meaning, as it is the altitude where rate of climb (ROC) becomes less than 0.5 m/s [6, 7].

There are also defined such concepts as speed of maximum endurance v_e , cruise speed v_{cr} , and speed of maximum range v_r . The maximum endurance speed and maximum range speed depend on fuel consumption characteristics of engine. The speed corresponding to the minimum hourly fuel consumption of engine is called speed of maximum endurance or economical speed. On the other hand, the speed corresponding to the minimum per-kilometer consumption of engine is the speed of maximum range and it is very close to the cruise speed (slightly more than cruise speed for real aircraft). The cruise speed is the speed at which the ratio of drag to speed is minimal, and can be found using Zhukovsky curves by drawing a tangent to the required thrust graph from the origin (**Figure 13**).

Let us now consider descending flight or glide (**Figure 14a**) and ascending (**Figure 14b**) flight of aircraft.

In descending flight, the throttle is usually set to minimum, so the thrust can be neglected and consider the gliding flight (**Figure 14a**), for which we can write down the following equations of force balance:

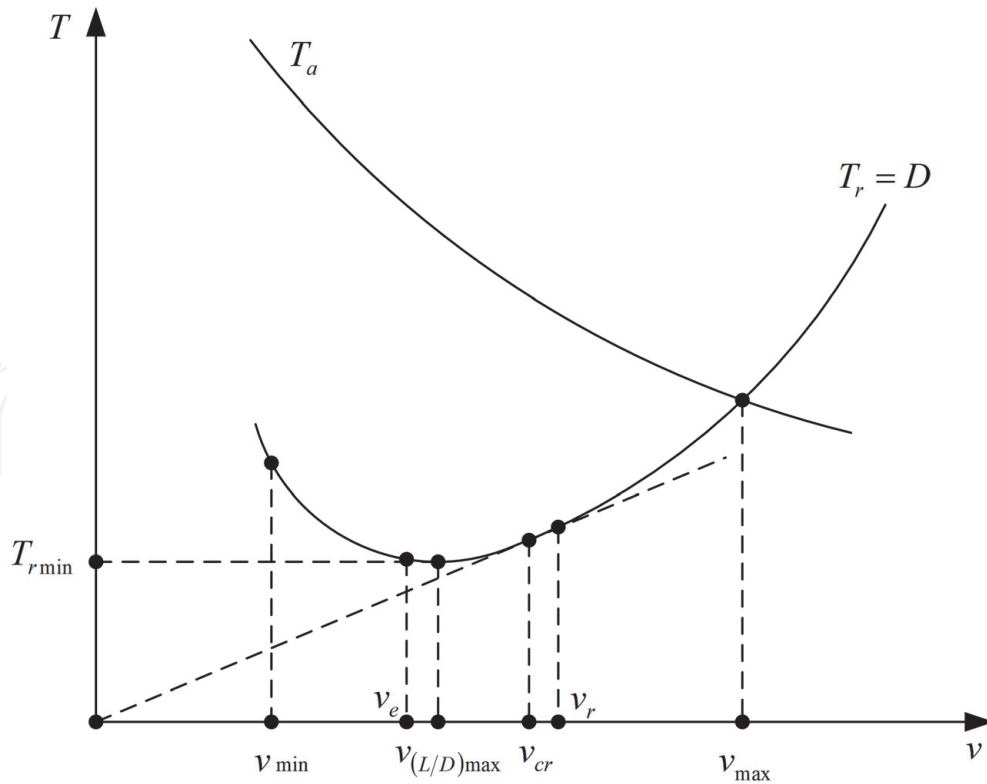


Figure 13.
 On cruise and other speeds.

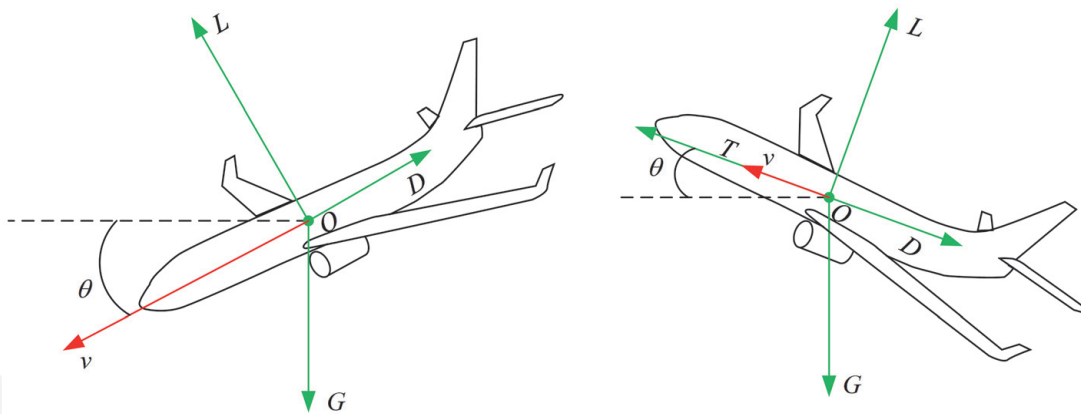


Figure 14.
 Force balance for descending and ascending flights. (a) Gliding flight; (b) ascending flight.

$$\begin{cases} L = G \cos |\theta|, \\ D = G \sin |\theta|. \end{cases}$$

where θ is the flight path angle.
 Based on the above we can get:

$$\tan |\theta| = \frac{D}{L} = \frac{1}{k}.$$

The flattest glide corresponds to the minimum magnitude of flight path angle $|\theta|_{min}$, which is case when the $\tan |\theta|$ is minimum, thus, we can write down the following:

$$|\theta|_{min} = \text{atan} \frac{1}{k_{max}}$$

The above means that the flattest glide, resulting the longest gliding distance, is also related to maximum lift-to-drag ratio k_{max} .

For the ascending flight the force balance is presented as follows:

$$\begin{cases} L = G \cos \theta, \\ T - D = G \sin \theta. \end{cases} \quad (7)$$

As we know, the rate of climb is the projection of airspeed to the vertical plane:

$$ROC = v \sin \theta.$$

From second equation of Eq. (7) we can get:

$$\sin \theta = \frac{T - D}{G},$$

or which is same as:

$$ROC = v \sin \theta = \frac{Tv - Dv}{G} = \frac{P_a - P_r}{G},$$

where $P_a = Tv$ is the available power, $P_r = Dv$ is the required power.

From the above we can find the maximum of ROC, that is, ROC_{max} corresponding to maximum of excess power $\Delta P_{max} = (P_a - P_r)_{max}$ (**Figure 15**).

The angle θ_{max} of steepest ascending flight can be found by dividing the ROC value by speed [9]:

$$\theta_{max} = \text{asin} \left(\frac{ROC}{v} \right)_{max},$$

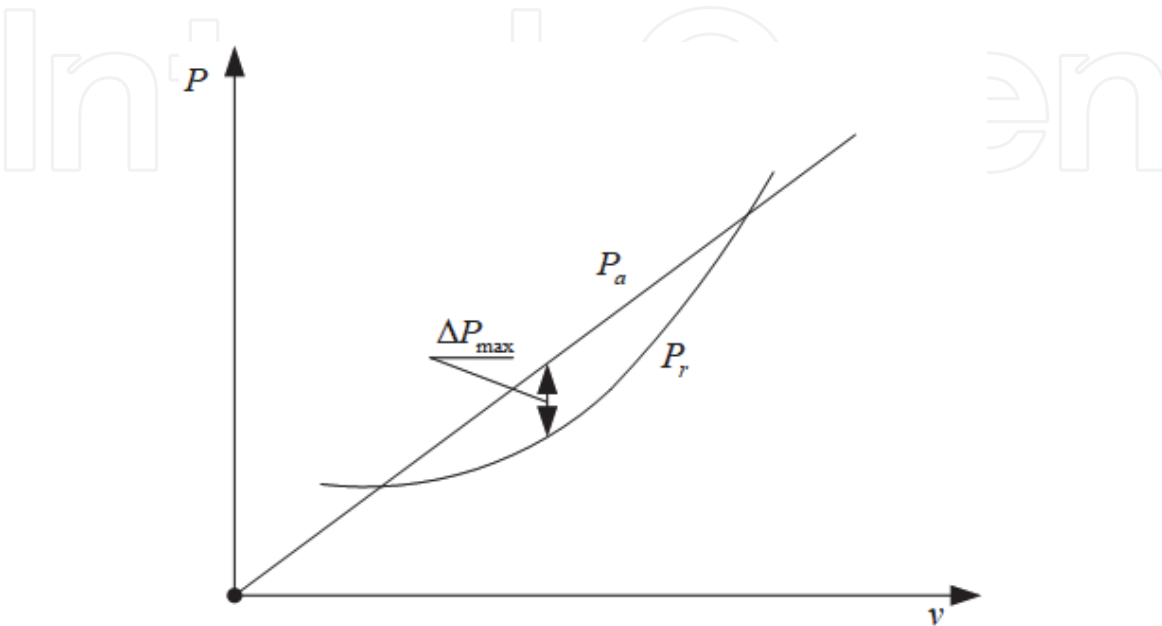


Figure 15.
Power diagram for jet aircraft.

which corresponds to

$$\theta_{\max} = \text{asin}\left(\frac{(T_a - T_r)_{\max}}{G}\right).$$

In ideal jet aircraft case, the angle of steepest climb is defined at the speed of maximum lift-to-drag ratio. The most economical ascending flight is defined by the operational regime of aircraft engine at which the minimum fuel will be consumed for aircraft to climb to the required altitude.

4. Flight envelope and operational limits of aircraft

For any aircraft, performance and operational limits are defined. Performance limits (**Figure 16**) are mostly defined by the aerodynamic configuration of aircraft. On the other hand, operational limits are based on the type of aircraft, structural and engine limits, wind resistance parameters, and maximum Mach number. All these limits are presented in diagrams of altitude h versus airspeed v and the final diagram, which represents the intersection of all limits, is called flight envelope (**Figure 17**). The flight envelope can be represented in graphs of altitude versus true airspeed, altitude versus indicated airspeed, or altitude versus Mach number.

All the speeds presented on **Figure 16** were described in the previous subsection. Operational limits related to the type of aircraft are described from the point of view of aircraft application: if an aircraft is a passenger jet, it should apply to the requirements of comfort for passengers and not exceed load factors of comfortable flight; on the other hand, if an aircraft is a jet fighter its operational limits from the point of view of load factors should be derived from compromise between the prevention of health issues of pilot that may occur and maneuverability for the combat use.

Structural limits are mostly related to aircraft strength, while the engine limits can be the result of its design and performance at higher altitudes. Wind resistance limits can be derived from the requirements of operational use or comfortability of flight for passengers.

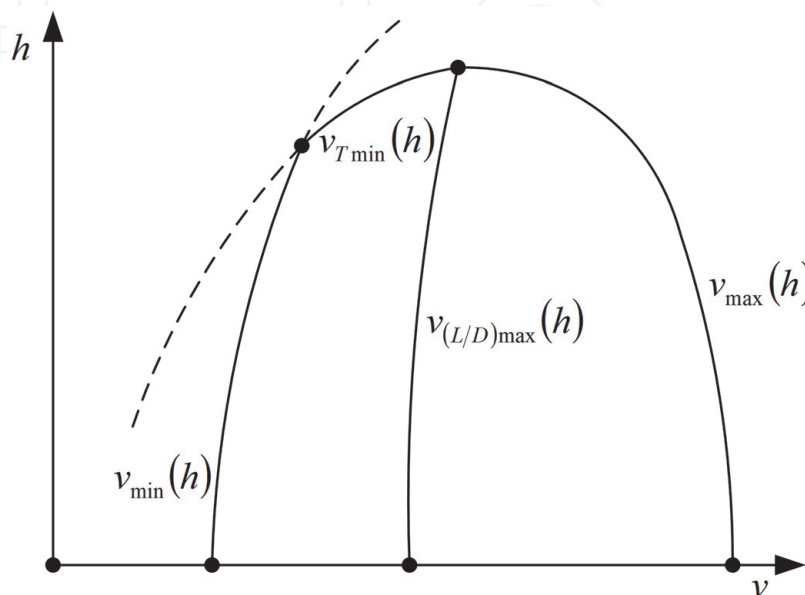


Figure 16.
 Performance limits.

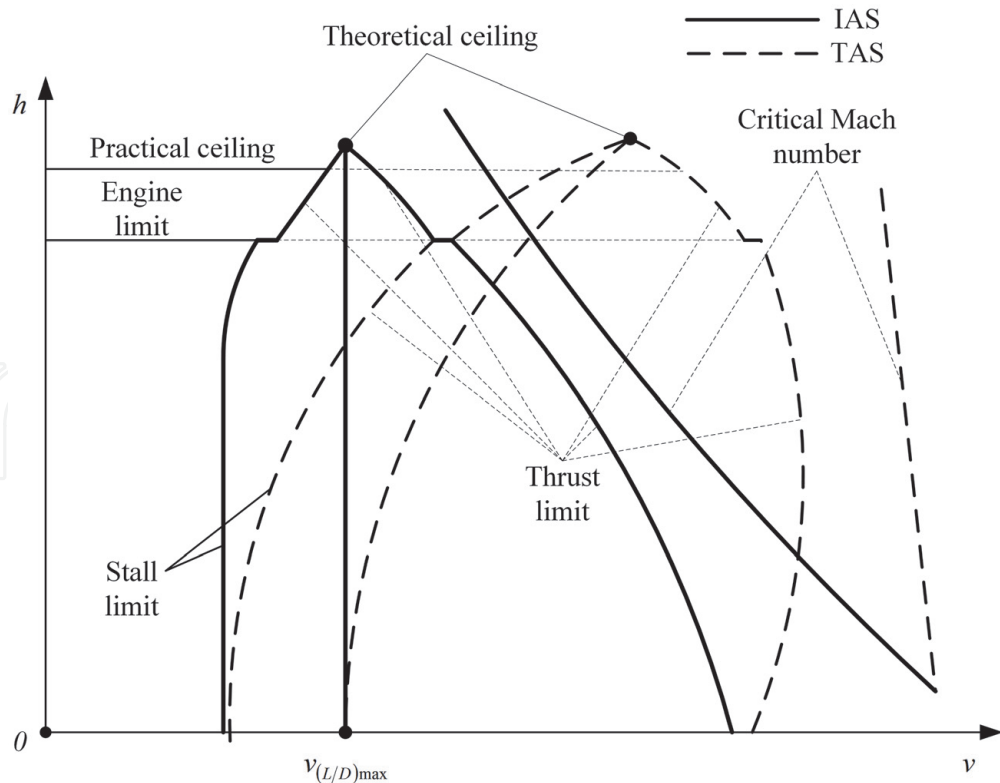


Figure 17.
Example of a flight envelope.

Maximum Mach number can be defined from the conditions of aeroelastic effects and vibrations, effects of shifting aerodynamic center, causing severe pitching moments, which can lead to the crashes, or losing effectiveness of aerodynamic surfaces. For example, for jet aircraft L-39 the critical Mach number is $M = 0.8$ and exceeding this condition leads to the shift of aerodynamic center of L-39, which generates pitching moment, causing a descending flight with acceleration [3]. To prevent such unstable flight, on L-39 air brakes are used, which automatically act at the Mach numbers $M = 0.78$. The critical Mach number is defined at airspeed flight that leads to generation of shock waves on the wing due to the acceleration of airflow on the upper surface of wing.

Finally, an example of flight envelope for analysis is presented in **Figure 17** where the intersection of all limiting conditions is described.

5. Conclusion

The material described in this chapter involves flight vehicle analysis using graphical and analytical tools for better understanding of the physical aspects of flight core parameters and development of strong and meaningful connections between them. The material from this chapter can be useful in the preliminary design and prototyping of flight vehicles and for finding the paths for further developments and improvements in the design.

Acknowledgments

In this work, the name of Prof. Nikolay Zhukovsky (January 17, 1847–March 17, 1921) is mentioned many times, while his name may be unfamiliar to many readers. Nikolay Zhukovsky was one of the first scientists who established the mathematical base of aerodynamics; he was the initiator and the first head of the Central

Aerohydrodynamic Institute (TsAGI), and on his initiative was created Zhukovsky Air Force Engineering Academy—alma mater of three famous Soviet aircraft designers Sergei Ilyushin, Artem Mikoyan, and Alexander Yakovlev.

Science lives in the research schools, and great scientists are those who both do great discoveries and develop the next generations of discoverers. Zhukovsky Air Force Engineering Academy is my alma mater as well, and with these few words I would like to express my appreciation to all my teachers who helped me on my way of professional and personal development.

IntechOpen

IntechOpen

Author details

Aram Baghiyan

Improvis Aerospace and Defense LLC, Yerevan, Armenia

*Address all correspondence to: abaghiyan@improvismail.com

IntechOpen

© 2020 The Author(s). Licensee IntechOpen. This chapter is distributed under the terms of the Creative Commons Attribution License (<http://creativecommons.org/licenses/by/3.0>), which permits unrestricted use, distribution, and reproduction in any medium, provided the original work is properly cited. 

References

[1] Lamar JE, Alford WJ Jr. Aerodynamic Center Considerations of Wings and Wing-Body Combinations. NASA Technical Note, TN D-3581; 1966. p. 16

[2] Drela M. Flight Vehicle Aerodynamics. Cambridge, Massachusetts: The MIT Press; 2014. p. 304

[3] Lysenko NM, editor. Practical Aerodynamics of Training Jet Aircraft. P. 2. Practical Aerodynamics of Aircraft L-39. Moscow: Voennoe Izdatelstvo; 1985. p. 248

[4] Clancy LJ. Aerodynamics. New York: Wiley; 1975. p. 172

[5] Korovin AE, Novikov YF. Practical Aerodynamics and Flight Dynamics of the Yak-52 and Yak-55 Aircraft. Moscow: DOSAAF; 1989. p. 357

[6] Kermode AC. In: Barnard RH, Philpott DR, editors. Mechanics of Flight (11th Edition)/Rev. London: Prentice Hall; 2006. p. 512

[7] Anderson JD. Introduction to Flight. New York: McGraw-Hill Education; 2016. p. 928

[8] Sloop JL. Liquid Hydrogen as a Propulsion Fuel. Washington, D.C.: NASA Scientific and Technical Information Office; 1945-1959, 1978. p. 338

[9] Smetana FO. Flight Vehicle Performance and Aerodynamic Control. Reston: American Institute of Aeronautics and Astronautics; 2001. p. 359